LWT - Food Science and Technology 184 (2023) 115065

Contents lists available at ScienceDirect

LWT

journal homepage: www.elsevier.com/locate/lwt

Quality assessment of 3D-printed cereal-based products

Nikolina Čukelj Mustač [a], Kristian Pastor [b], Jovana Kojić [c], Bojana Voučko [a], Duška Ćurić [a], João Miguel Rocha [d,e,f,*], Dubravka Novotni [a]

[a] Faculty of Food Technology and Biotechnology, University of Zagreb, Pierottijeva 6, 10000, Zagreb, Croatia
[b] Faculty of Technology Novi Sad, University of Novi Sad, Bul. cara Lazara 1, 21000, Novi Sad, Serbia
[c] Institute of Food Technology in Novi Sad (FINS), University of Novi Sad, Bul. cara Lazara 1, 21000, Novi Sad, Serbia
[d] Universidade Católica Portuguesa, CBQF - Centro de Biotecnologia e Química Fina – Laboratório Associado, Escola Superior de Biotecnologia, Rua Diogo Botelho 1327, 4169-005, Porto, Portugal
[e] LEPABE—Laboratory for Process Engineering, Environment, Biotechnology and Energy, Faculty of Engineering, University of Porto, Rua Dr. Roberto Frias, s/n, 4200-465, Porto, Portugal
[f] ALiCE—Associate Laboratory in Chemical Engineering, Faculty of Engineering, University of Porto, Rua Dr. Roberto Frias, s/n, 4200-465, Porto, Portugal

ARTICLE INFO

Keywords:
Dough
Rheology
Printability
End-product analysis
Structure stability

ABSTRACT

The process of three-dimensional (3D) printing is of greatest interest to food science and engineering community because it offers numerous opportunities for innovative food design, new product formulations and personalized nutrition. Of particular interest are food inks based on cereal flours or starches, whose unique rheological properties make them suitable for 3D printing, typically with an extrusion-based printer. While the factors that influence the success of food printing are well addressed, the terminology and methods used to evaluate the process and product features are miscellaneous.

Therefore, this research work aims at providing an overview of the most commonly used parameters and methods for evaluation of the extrusion-based 3D printing process and the resulting cereal-based foods. Physical and sensory methods that are successfully used for the quality assessment of the ink and the printed raw objects, as well as the post-processed products are here reviewed and outlined. The properties of inks, usually determined with dynamic rheological tests, are linked to various aspects of printing quality whereas the physical properties of printed raw forms are usually evaluated by image analysis combined with mathematical calculations. Microscopy analysis is undertaken to study the microstructure of both the raw objects and the end-products, while texture analysis and sensory evaluation of final product are performed both by a panel and instrumentally. We provide details of the tests, but also emphasize the need to standardize the procedures and terminology in order to avoid misunderstandings and multiple variations of similar methods. This review provides a basis for further development and standardization of the methodology for quality assessment of 3D-printed cereal-based foods.

1. Introduction

Three-dimensional (3D) food printing was introduced to food scientists and engineers in 2007. Since 2016, the number of publications on that topic has increased steeply (Zhang, Pandya, McClements, Lu, & Kinchla, 2022) including the application of cereal flour and/or starch. Nevertheless, it is still a perspective field for research, since in the Web of Science Core Collection the number of publications containing the terms [("additive manufacturing" OR "3D printing" OR "three dimensional printing") AND "cereal"] from 2007 to date is 81, with a majority of 58 documents published since 2018.

Cereal-based material (dough, paste, batter) is naturally printable material due to its ability to withstand the 3D shape. Besides, cereal products have always been a good vehicle for nutrient fortification due to their daily use and rather neutral flavour. Although not all steps are always considered, a common approach in printing cereal-based foods is to: (i) mix the ingredients with water, taking into account their chemical/physical properties (*e.g.*, particle size); (ii) evaluate rheological properties; (iii) computer design a desired shape and adjust parameters of printer which is usually extrusion based (*e.g.*, printing speed, movement, filament load, nozzle properties, infill level); (iv) evaluate flowability, extrudability, formability of material; and (v) evaluate post-

* Corresponding author. LEPABE—Laboratory for Process Engineering, Environment, Biotechnology and Energy, Faculty of Engineering, University of Porto, Rua Dr. Roberto Frias, s/n, 4200-465, Porto, Portugal.
E-mail address: jmfrocha@fc.up.pt (J.M. Rocha).

https://doi.org/10.1016/j.lwt.2023.115065
Received 20 March 2023; Received in revised form 4 July 2023; Accepted 6 July 2023
Available online 14 July 2023

processing product stability (Derossi, Caporizzi, Oral, & Severini, 2020a; Habuš et al., 2022a; Lille, Nurmela, Nordlund, Metsä-Kortelainen, & Sozer, 2018; Pulatsu, Su, Lin, & Lin, 2020).

Various quality assessment methods are used to investigate a success of 3D printing process, as well as to generate meaningful data for further process development on a pilot or an industrial scale. In general, the quality of 3D-printed foods is influenced by numerous factors, which can roughly be divided into those affected by printer settings, printing material and post-processing methods. The first two complement each other to achieve maximum precision, multiple layers, and minimal deformation (Derossi, Caporizzi, Oral, & Severini, 2020). Printer settings are the technical aspects of 3D printing related to the characteristics of the printer, as well as the supporting slicer and software, which have been discussed elsewhere (Derossi, Caporizzi, Ricci, & Severini, 2019). The quality of cereal-based 3D-printed materials and end-products are commonly assessed by rheology measurements, digital imaging, texture and sensory analyses, and mathematical calculations (Fig. 1). Understanding dough rheology in relation to printing behaviour is important since its specific viscoelastic and plastic properties change with shear, time, and temperature depending on its composition (Liu, Bhandari, Prakash, Mantihal, & Zhang, 2019). Further, digital images of printed lines/shapes provide an insight into the extent to which the shape is confined to the defined dimensions, and can be related to material rheology. Nevertheless, a better understanding of rheology to predict the success of the entire printing process, from extrusion to the self-supporting phase, is ongoing research (Cheng et al., 2022).

Most cereal-based materials require post-processing, which can lead to deformation (Habuš et al., 2021; Keerthana, Anukiruthika, Moses, & Anandharamakrishnan, 2020; Lille et al., 2018) and understanding structural stability during post-processing is critical for integrating 3D printing into thermal processes. Various factors and methods are used in the literature to define the quality of 3D-printed products, but require detailed description and systematization to maximize their utility. Indeed, the lack of a classification system for bio ink printability is a problem pointed out already by Gillispie et al. (2020). In this context, this is a review of the most common methods for qualifying cereal material and cereal-based 3D-printed products. The aim is to fill the gap in literature by providing a basis for classification of methods and terminology used and to identify the numerous variations of similar parameters and methods.

2. Rheology testing

Cereal-based material needs to have specific rheological properties to be easily extruded through the nozzle tip without breakage, rapidly go through the gelation process once 3D-printed and have sufficient mechanical strength to resist deformation. According to Liu et al. (2019), three stages of the printing process are linked to the corresponding rheological properties: (i) extrusion stage to yield stress, viscosity and shear-thinning behaviour; (ii) recovery stage to shear and temperature recovery properties; and (iii) self-supporting stage to complex modulus and yield stress at room temperature. Similarly, Maldonado-Rosas et al. (2022) examined the before-extrusion stage with flow initiation analysis and shear thinning behaviour, the during-extrusion stage with temperature sweep test, and the post-extrusion recovery stage through shear recovery behaviour.

A common choice for cereal-based ink rheology testing is the oscillatory rheometer, with two parallel plates and up to a 2 mm gap (Habuš et al., 2022a; Liu et al., 2019; Maldonado-Rosas et al., 2022; Vieira et al., 2020), although rotational instruments are used as well (Vukušić Pavičić et al., 2021; Heckl, Korber, Jekle, & Becker, 2023). Besides, cereal materials are often analysed with texture analysers using texture profile analysis (Keerthana et al., 2020; Vieira et al., 2020).

Rheometers provide variety of parameters (Table 1) via different tests commonly conducted in triplicate, after mixing and resting, few minutes to hours before measurement (Pulatsu et al., 2020; Vieira et al., 2020). The first step in a rheological characterization is the determination of linear viscoelastic region (LVER), using an amplitude sweep test. Further characterization includes determination of storage G′ and loss G'' moduli through amplitude (strain or stress), frequency, or temperature sweep tests, as well as calculation of complex G* modulus and (tangent) phase angle (δ) (Table 1). Flow of cereal-based material from the printer nozzle is commonly related to the flow stress (or the flow point) which is sometimes referred to as yield stress, despite the distinction between the two (Lille, Kortekangas, Heiniö, & Sozer, 2020) (Table 1). Continuity of a material flow depends on its viscosity under given conditions, mainly temperature and shear rate (Maldonado-Rosas et al., 2022). Hence, materials with higher viscosities will create higher friction in the printer, while excessively low viscosity can lead to difficulties in shaping (Cheng et al., 2022). A frequently used model for fitting viscosity data over shear rate/stress to describe shear behaviour is the two-parameter Power law model (Table 1) (Liu et al., 2019). Yet, this model is not suitable for some materials in the low-shear and high-shear ranges, in which case Cross equation considering zero-shear viscosity, Sisko equation (Cheng, 2022), or Bird-Carreau model (Guo et al., 2020) might be more useful. Shear thinning behaviour is desirable as it allows the printing material to become thinner when experiencing a higher shear rate, resulting in smooth flow out of a printing nozzle (Guo et al.,

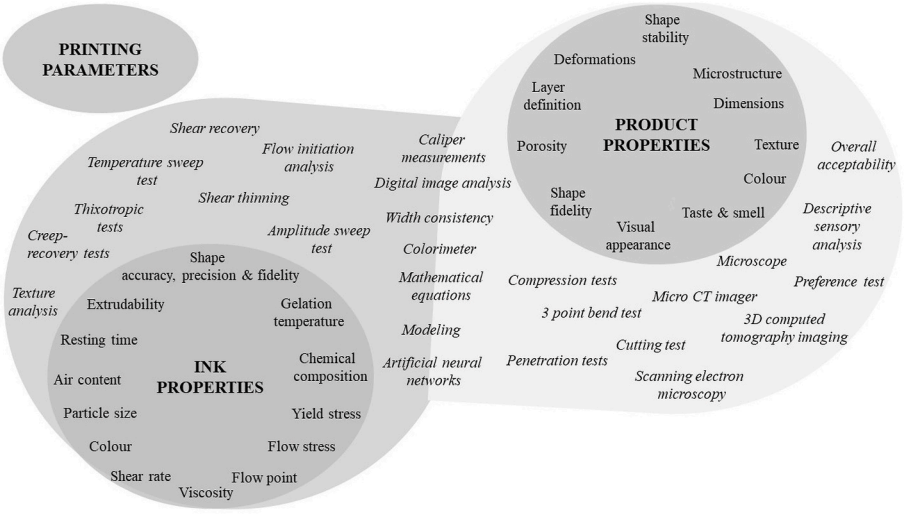

Fig. 1. Key parameters affecting the quality of 3D-printed products and methods for determining quality of cereal-based 3D-printed products.

Table 1
Rheological parameters relevant for extrusion-based 3D-printing of cereal material (adapted from Sahin & Sumnu (2006) and Mezger (2015).

Parameter (symbol, unit)	Description	Calculation	Significance in 3D printing of cereal-based ink
Linear viscoelastic region (LVER, % strain)	*area indicating the range in which test can be carried out without destroying the material structure; determined in an oscillatory measurement with increasing stress or strain amplitude at a constant frequency (amplitude sweep tests)*	The limit of LVER (linearity limit) can be determined with a ruler, software or the data table	- solid-like behavior in the LVER is necessary for extrusion-type 3D printing (Pulatsu et al., 2020)
Shear rate ($\dot{\gamma}$, s^{-1})	*change in velocity of a material per unit distance in the direction perpendicular to the direction of the applied shear stress; measure of the rate at which material is deforming due to applied shear stress*	$\dot{\gamma} = \frac{v}{h}$ where v = velocity (m/s), h = shear gap (m)	- in oat flour dough with microalgae critical shear rate (ẏ), that is, onset shear rate for shear thinning behavior highly correlated (0.941) with printability levels (Oliveira et al., 2022)
Shear modulus (G, Pa)	*modulus of rigidity – describes the relationship between shear stress and strain; slope along the linear portion of the stress–strain curve*	$G = \frac{\tau}{\gamma} = \frac{F/A}{s/h}$ where τ = shear stress (N/m^2 (Pa)), γ = shear strain (%), F = shear force, A = shear area, s = deflection path, h = shear gap	- higher shear modulus - better shape retention (baking stability) but difficult and non-uniform extrusion and low resolution of printed objects and hard texture of cookies (Kim et al., 2019)
Phase angle (δ, ∘)	*phase difference between the applied deformation and the resulting material response*	If closer to 90° material is more liquid, if closer to 0° material is more solid	- despite similar phase angle values pastes made from starch, milk powder, cellulose nanofiber, rye bran, oat protein and faba bean protein concentrate had different shape stability after printing (Lille et al., 2018) - lower phase angle is beneficial for print shape stability of paste from milk powder and wholegrain rye flour (Lille et al., 2020)
Storage (elastic) modulus (G′, Pa)	*elastic portion of viscoelastic behaviour, i.e. solid-state behaviour*	G' = (τ/γ) × cos δ, where γ = shear strain, τ = shear stress, δ = phase angle between G'' and G′	- high G′ indicates difficult extrusion at start; low G′ indicates structure collapse (Huang et al., 2020) - G′ values between 1000 and 8000 Pa yield good printability and post-printing dimensional stability of pastes from wholegrain rye flour with milk powder (Lille et al., 2020) - the printing quality of wheat flour dough with added sucrose and oil is satisfactory even in the wider range of G′ values (3800–12000 Pa) (Masbernat et al., 2021) - G′ highly correlates with printability level (r = 0.958) of doughs from oat flour with added microalgae: G′ values up to 4.2×10^4 Pa are satisfactorily printed (level 1 printability); G′ values 6.1×10^4 Pa and 8.1×10^4 have low flowability and not well defined shape (level 2 printability); G′ values ($>1.1 \times 10^5$ Pa) are not unprintable and cannot flow through nozzle (level 3 printability) (Oliveira et al., 2022) - G′ alone is not sufficient to correctly predict the printing accuracy of cereal-based inks from wheat starch, soy protein isolate and hydrocolloids but the yield stress needs to be considered (Heckl et al., 2023)
Loss (viscous) modulus (G'', Pa)	*viscous portion of viscoelastic behaviour, i.e. liquid-state behaviour*	G'' = (τ/γ) × sin δ (as for G′)	- decrease in G" is highly beneficial for shape stability during printing of paste from wholegrain rye flour and milk powder (Lille et al., 2020) - printability and G″ of oat flour doughs with added microalgae highly correlate (r = 0.951) (Oliveira et al., 2022)
Loss (damping) factor (tan δ, ∘)	*tangent of phase angle δ, index of the relative elastic or viscous nature; when tan δ > 1, a material predominantly exhibits viscous characteristics and when tan δ < 1, a material tends to exhibit a solid-like behaviour with poor fluidity; also phase transition or gel point.*	tan δ = G''/G′	- tan δ is a relevant additional indicator to predict the printing quality of wheat flour doughs with added sucrose and oil: the printing quality is high with tan δ in range 0.14–0.17, while poor printability quality is at tan δ 0.20 (Masbernat et al., 2021)

(*continued on next page*)

Table 1 (*continued*)

Parameter (symbol, unit)	Description	Calculation	Significance in 3D printing of cereal-based ink
			- higher tan δ values of buckwheat starch-pectin gels indicate changes from elastic to more plastic behavior, which is beneficial for extrusion-based 3D printing (Guo et al., 2020) - printability and tan δ ranging from 0.18 to 0.21 highly correlate (r = 0.816) (Oliveira et al., 2022)
Apparent viscosity (or consistency) (η, Pa·s)	*ratio between the shear stress and shear rate; used for non-Newtonian fluids*	$\eta = \tau/\dot{\gamma}$, where τ = shear stress and $\dot{\gamma}$ = shear rate	- high apparent viscosity indicates difficult extrusion at start while low apparent viscosity indicates structure collapse of brown rice gel (Huang et al., 2020)
Complex viscosity (η*, Pa·s)	*viscosity obtained in an oscillatory test, measured in a steady shear test*	$\eta^* = \eta' + i\,\eta''$, where $\eta' = G''/\omega$, $\eta'' = G'/\omega$ or $\eta^* = G^*/\omega$, where G^* = complex modulus; $G^{*2} = G'^2 + G''^2 = \tau_A/\gamma_A$, ω = angular frequency (rad/s) and τ_A = shear stress amplitude (Pa), γ_A = strain amplitude (dimensionless or %)	- complex viscosity can be predictor of printing precision and shape shrinkage of snack made from oat/barley flour, pea protein and wheat bran; shape deformation of snack inversely correlates with the complex viscosity of the dough (Habuš et al., 2021, 2022) - gluten-free batters with the highest values for complex viscosity (5368.90 Pa s) are the most accurately printed (Radoš et al., 2023)
Zero-shear (or steady state) viscosity (η_0, Pa)	*viscosity measured at very low shear rates e.g. below 1 s^{-1}, recognized as the material viscosity at rest, indicating resistance to deformation under long-term load;*	$\eta_0 = \tau/\dot{\gamma}$ where τ = shear stress, $\dot{\gamma}$ = low shear rate	- the value can be related to the stability of a printed object (Guo et al., 2020) - η_0 highly positively correlates (r = 0.928) with printability of oat flour doughs with microalgae addition (Oliveira et al., 2022)
Yield stress (τ_y, Pa)	*lowest shear-stress above which material will behave like fluid and below which will act like a (soft) solid material; preferably determined with controlled shear stress test; used to determine the limit of linear-elastic region (linearity limit)*	By analysis of γ/τ diagram (deformation/shear stress): logarithmic scale with the shear stress plotted on x-axis, by application of straight fitting line in the linear-elastic deformation region, or with the "tangent crossover method"; point where the deformation starts to deviate from the straight line	- generally used to evaluate extrudability of food material, but does not guarantee printability and should be combined with other tests, *e.g.* frequency sweep, creep recovery (Kim et al., 2019; Pulatsu et al., 2021) - related to the ability of the material to keep its shape under gravity and under the stresses generated by material layers deposited on top of it (Lille et al., 2018) - corresponds with the extrudability and mechanical strength of wheat or rice or tapioca cookie dough; too low yield stress values are incompatible for printing of cookie dough since they could not keep their shape as expected (Pulatsu et al., 2020) - shape deformation of snack is inversely correlated with the yield stress (r = 0.76) of the oat/barley flour, pea protein and wheat bran dough (Habuš et al., 2021) - higher yield stress is beneficial for shape stability of printed paste from wholegrain rye flour and milk powder (Lille et al., 2020) - lower yield stress is a desirable since extrusion stops and starts often during the printing, but if too low it may cause ink leakage from the nozzle or if too high would lead to difficult and unsmooth printing, asking of more robust printer that can generate larger force in a controlled way (Cheng et al., 2022; Liu et al., 2019) - the stability after printing paste from wheat starch, soy protein isolate and hydrocolloids is improved by their high yield stress (Heckl et al., 2023)
Flow point/stress (τ_f, Pa)	*minimum pressure needed to initiate the flow of the material*	Cross-over point of G′ and G″ curve when observed in a relation to the applied shear stress; dependent on the measuring conditions	- flow point has great influence on printing quality of oat flour, pea protein and wheat bran dough (Habuš et al., 2022a) - lower flow point in buckwheat starch-pectin gels should exhibit higher printability (Guo et al., 2021)

(*continued on next page*)

Table 1 (*continued*)

Parameter (symbol, unit)	Description	Calculation	Significance in 3D printing of cereal-based ink
Behaviour under changing shear rates	*changes of the viscosity of material (thinning or thickening) with increasing shear rate; data can be fitted to power law model which assumes that the material viscosity is proportional to the rate of shear to a power, typically represented by the symbol n; data can be fitted to Cross-Williamson non-linear model for shear-thinning materials*	Power law model: $\eta = K\dot{\gamma}^{(n-1)}$, where K = consistency index ($Pa*s^n$), n = flow behavior index, $\dot{\gamma}$ = shear rate (Guo et al., 2021) Cross-Williamson non-linear model: $\eta = \frac{\eta_0}{1+(\lambda \times \dot{\gamma})^m}$ where η_0 (Pa.s) = zero-shear rate limiting viscosity, λ (s) = time constant, m = dimensionless shear-thinning index (Oliveira et al., 2022)	- shear thinning is inverse to flow index (n); $n < 1$ is required in most cases of edible ink printing which together with low K indicate a low pressure to obtain a continuous flow; if $n < 1$ fluids shear thin, weak shear thinning behavior can be observed within $n \sim 0.6$, and highly shear thinning is presented with values of $n \leq 0.2$ (Huang et al., 2020; Liu et al., 2019; Maldonado-Rosas et al., 2022) - n is generally the key performance index of printing (Cheng, 2022); - lower consistency index (K) positively correlates with the viscosity and indicates easier extrusion and higher printing accuracy; flow index (n) negatively correlates with the viscosity and describes pseudo-plasticity material behaviour during application of shear, whether it thins, thickens or the shear has no influence on the viscosity; lower flow point indicates higher printability (Guo et al., 2021) - m shear-thinning index highly correlates with printability levels of oat flour doughs with microalgae addition ($r = 0.774$) (Oliveira et al., 2022)
Temperature dependent behaviour	*determined with temperature sweep tests in which shear conditions (shear stress/strain amplitude, frequency) are kept constant, while temperature changes according to previously defined profile; useful for determination of gelation temperature (T_{gel}) and gelation time (t_{gel}).*	T_{gel} = from temperature ramp-down curve by extrapolating the high and low temperature asymptotes of the viscosity and specifying the temperature at which these intersect; t_{gel} = time necessary to reach G* plateau; point at the crossover point of two tangents fitted to the plateau-region and G*-increase regions of the curves at room temperature	- useful in predicting deformation over a wide temperature range during the baking process (Kim et al., 2019) - a change in G′, G″, G*, and tan δ of wheat flour cookie dough over temperature increase is detected due to the fat melting, the pyrolytic decomposition and leaching of the amylose in flour starch granule (Kim et al., 2019; Vieira et al., 2020), as well as in oat flour, pea protein and wheat bran dough (Habuš et al., 2022) - gelation time is a critical parameter for the shape retention of extruded filaments and final printed objects since long gelation time would cause the spreading deformation of printed objects due to insufficient mechanical strength within a short time of extrusion (Liu et al., 2019)
Thixotropic behaviour	*structural deformation and regeneration; behaviour (time-dependent) characterized by a decrease in the values parameters (e.g. shear viscosity, storage modules) against a constant, time-independent limiting value (e.g. shear stress or rate) and the complete time-dependent recovery of the initial state upon reduction of the load; determined with 3-interval thixotropy test (3ITT)*	Recovery index = $\frac{\eta_\infty - \eta_{shear}}{\eta_0 - \eta_{shear}} \times 100$ where η_0 = final viscosity of the first low oscillation, η_∞ = the final equilibrium apparent viscosity of the second low oscillation; η_{shear} = the final apparent viscosity of the high shear stage (Maldonado-Rosas et al., 2022); % Recovery = $\frac{G_t'}{G_1'} \times 100$ where G'_1 (Pa) = storage modulus at the first interval, G'_t (Pa) at different times during the third interval (Heckl et al., 2023)	- test allows to imitate the mechanical conditions occurring during the 3D printing process of cereal-based inks from wheat starch, soy protein isolate and hydrocolloids; the stronger the network within the system the smaller the influence of the shear stress during the extrusion and faster the recovery; the structural recovery and the stack height after printing are highly correlated (Heckl et al., 2023) - thixotropic behaviour is highly desirable as it enables easier extrusion out while rapid recovery to ensure sufficient mechanical strength needed to support the following extruded layers (Liu et al., 2019; Maldonado-Rosas et al., 2022) - G'_t is related to the difficulty of material extrusion with lower values indicating smoother ink extrusion (Ji et al., 2023)
Creep recoverability	*the ability of the material internal structure to resist sliding deformation by first applying shear stress beyond LVER for a pre-established time-period, and then by releasing of applied stress to recover the ink; the resulting strain is measured as a function of time needed for ink to recover*	Commonly by fitting creep compliance values to the four parameter Burger's model $J(t)_c = J_0 + J_m\left(1 - \exp\left(\frac{-t}{\lambda}\right)\right) + \frac{t}{\eta_0}$ $J(t)_r = J_{max} - J_0 - J_m\left(1 - \exp\left(\frac{-t}{\lambda}\right)\right)$ Where J_0 (Pa^{-1}), J_m (Pa^{-1}), and J_{max} (Pa^{-1}) = instantaneous, viscoelastic, and maximumum creep compliance values, respectively; t (s) = phase time, λ (s) = average retardation time, η_0 = viscosity coefficient (Pa s)	- little or no (elastic) recovery after applied stress indicates that wheat or rice or tapioca cookie dough is unsuitable for 3D printing (Pulatsu et al., 2021) - in wheat flour cookie dough with microalgae, the higher the steady-state viscosity, the higher the resistance to deformation; more stiff doughs take longer to deform and to recover their structure (Vieira et al., 2020)

2020).

In temperature sweep test, intersection of G′ and G′′ (transition temperature) indicates an alteration of material structure, and is associated with gelling, denaturation, or glass transition. To set a proper printing temperature, it is important to determine gelation temperature (T_{gel}) (Table 1). Generally, it is recommended that the nozzle cavity temperature is higher than T_{gel} to compensate for the system heating loss (Cheng, 2022), and to ensure both an easy extrusion of material and a rapid gelation to form sufficient self-supporting strength once extruded from the nozzle tip (Liu et al., 2019). Hence, temperature control allows the edible ink to be printed into a desirable structure, while avoiding potential unnecessary side effects including denaturation, colour fading or darkening (Habuš et al., 2021).

While G′ and G′′ in stress sweeps describe the structural strength or mechanical rigidity of the material at rest, they might not be precise enough for affirmation of sufficient mechanical strength needed to retain the deposited shape. To analyse material recovery after extrusion, a three-step recovery test, further extended to a time-dependent shear test, can be conducted to observe if the formulations remain stable over an extended printing time under the same shear rate (Maldonando-Rosas et al., 2022).

Thixotropic tests are helpful to predict printing and post-printing behaviour of a cereal material. First, a low shear rate is applied, corresponding to the slow flowing of the ink in the syringe before printing. Second, the shear rate strongly increases within a short period of time, simulating the printing process, which can lead to a sharp decrease in viscosity indicating the disruption of the entanglements or cross-links between polymer chains. In the third stage, the shear rate returns to the low values, allowing for a gradual building up of molecular structures and a recovery of viscosity, mimicking the post-printing stage. Since time is crucial for obtaining a desired mechanical strength and an accurate geometry, one should keep in mind the time needed to recover to constant viscosity (Cheng et al., 2022).

The creep-recovery test reflects the ability of the internal structure to resist sliding deformation and enables measuring the destruction and restoration of material. Fitting the data to the Burger's model results in calculation of the zero-shear rate viscosity, that explains the resistance towards deformation under long term loading. With faster recovery a higher shape fidelity is expected, while less strain in the test indicates a stronger ability of the material to maintain the printed shape and structure, but also higher extrusion rates. It mostly correlates with the stability of the 3D-printed structure (Vieira et al., 2020; Cheng, 2022).

Yield stress can also reflect the supporting strength of stacked layers after extrusion. In that sense, yield stress should be observed not under temperature of printing (in which case it gives an indication of extrusion properties) but at room temperature, to give indications of properties during the post-printing period. Namely, yield stress is related to temperature in an inversely proportional manner (Liu et al., 2019).

While rheological properties expressed for example through printability maps (Oliveira, Sousa, & Raymundo, 2022), are a key indicator of the 3D printability (Guo, Zhang, & Devahastin, 2020), food materials are subjected to different shear and deformation forces during extrusion through the printer nozzle tip, then in the rheometer. Thus, the prediction of the material printability by rheological measurements might be less straightforward than anticipated and subjected to interpretation. Also, one must not forget that other factors, such as homogeneity, particle size, air content of printing paste, water distribution in printing paste, as well as structural properties of cereal raw material, such as degree of starch branching, contribute to the quality of the printed filament (Ji et al., 2022; Ji et al., 2023; Lille et al., 2020; Radoš et al., 2023). Advanced statistical methods, such as artificial neural networks, showed that dough rheological properties, particularly flow point but also complex viscosity, yield point, breakdown and maximum hot viscosity, can be used to predict the shrinkage and colour of 3D-printed snacks (Habuš et al., 2022a).

3. 3D print quality

Print quality is highly dependent on the material printability. While the term printability is very broad, we will refer to Gillispie et al. (2020) who defined printability as "the ability of a material, when subjected to a certain set of printing conditions, to be printed in a way which results in printing outcomes desirable for a given application". Common printing outcomes related to cereal-based material are: manageability and uniformity of extrusion, line dimensions and their preservation upon extrusion, precision, accuracy and/or fidelity of the 3D-printed shape, and shape stability (Table 2).

Extrudability can be assessed qualitatively (visually), by analysis of uniformity and consistency of an individual straight lines or for example, by observing overlaps in pentagrams of different angles (Liu et al., 2019). High quality digital images of the printed lines are a prerequisite for qualitative or quantitative assessment of extrudability. For example, Ma, Schutyser, Boom, & Zhang (2021) photographed lines 10 s after extrusion, on a black background beside a white ruler, from a 40 cm distance, using a macro lens and denoised images by the Gaussian blur algorithm. Fahmy, Becker, & Jekle (2020) proposed a method with on-board cameras and a light system to obtain images further evaluated in MATLAB using image analysis algorithms. They proposed more complex quantitative methods for evaluation of printed line dimensions, taking into account areas of over-extrusion and under-extrusion (Table 2, equations 1-3), as well as to estimate the initial delay in extrusion. Ma et al. (2021) predicted the extrudability of complex food materials during 3D printing using image analysis. Although they did not measure the extrudability of cereal-based material, we anticipate that the proposed methods could be applied for cereal material as well. For example, width consistency index can be calculated as a proportion of the width distribution measured within ±5% of the model line width, while line height is estimated by approximating the cross-sectional area of the extruded line as flattened tube (Table 2, equation 4). Line diameter can be predicted from volume and area of the line assuming elliptical cross-section (Huang, 2018). Line spread factor can be calculated as a ratio of line width to height and represented as the normalized to the ideal value (Vukušić Pavičić et al., 2021). Generally, in 3D printing, up to 70% of line width expansion ("die swell") is considered acceptable when generating a printing path from the digital design (Ma et al., 2021). Vukušić Pavičić et al. (2021) considered acceptable if the diameter of a printed line was up to 130% nozzle diameter whereas line height can range between 60 and 80% of nozzle diameter (Ma et al., 2021).

Properties of a printed line (1D), together with those determined on two dimensional planar structures (2D, up-to three layers), indicate the feasibility of 3D structures. An inevitable problem with 3D printing quality assessment methodology is the use of multiple terms or measurement methods for the same property or vice-versa, *i.e.* the use of the same term for different properties. For example, a feature describing the similarity of measured printed object dimensions (diameter, width, length, height, surface area) to the designed object measures is known as printing precision, accuracy, fidelity, and integrity index (Table 2, equations 5-7). However, it is necessary to distinguish between those terms. While precision and accuracy both refer to the process error, accuracy would be as Gilispie et al. (2020) defined it, a similarity of a 3D-printed construct to the intended computer design, with respect to the printing parameters used (Heckl et al., 2023; Huang, Zhang, & Bhandari, 2019). Precision on the other hand is independent on the accuracy and shows how the measured dimensions of the same objects are close to each other. It might be calculated by comparing individual shape dimensions to the last printed shape which is considered the most accurately or ideally printed (Vukušić Pavičić et al., 2021). Although it could refer to accuracy, precision was often estimated as an area of single layer (usually top filament) relatively to the area of designed model (Huang, Zhang, & Guo, 2020) or relatively to the nozzle diameter (Keerthana et al., 2020; Habuš et al., 2021) (Table 2, equations 5 and 6).

Finally, shape fidelity would be an ability of ink to maintain the shape upon its deposition, which is commonly determined by measurement and comparison of top line dimensions (e.g., width, height, diameter, or area) to theoretical dimensions (Table 2, equation 7). Nijdam, Agarwal, & Schon (2021) proposed Buckingham-π method to plot a window of dimensional stability of 3D-printed food structures considering various factors.

Height, width, thickness, and diameter of 3D-printed object can be measured with a calliper (Pulatsu et al., 2020) at multiple positions, preferably in ten replicates (Fig. 2) (Derossi, Caporizzi, Paolillo, & Severini, 2021; Liu et al., 2020a). Since cereal-based inks are easily deformed during manipulation, objects can also be photographed or scanned immediately or after freezing (Severini, Azzollini, Albenzio, & Derossi, 2018). Photographs are taken from top and lateral positions using a high-resolution camera beside a ruler (Derossi, Caporizzi, et al., 2020; Huang et al., 2019; Liu et al., 2019). After calibration, in addition to dimensions such as width and length, area can also be estimated using software tools, e.g., ImageJ (Derossi, Caporizzi, et al., 2020; Guo, Zhang, & Devahastin, 2021; Liu et al., 2019; Vukušić Pavičić et al., 2021). Moreover, a 3D computed tomography imaging was proposed (Severini et al., 2018). Visual assessment of photographs on a scale from 1 to 5 (Lille et al., 2018) can be also employed, as well as visual sensory analysis to hedonically rate appearance, shape, layer definitions, dimensional stability, binding property, texture and finishing, and thread quality of 3D-printed object (Theagarajan, Moses, & Anandharamakrishnan, 2020).

In addition, critical height which is the maximal height reached in printing before collapse of a designed shape, indicates the quality of multiple layers stacking which can be linked with material rheology. Height can also be used to assess kinetics of printing through video recording of the process and fitting the data to **equation 8** (Derossi, Caporizzi, Azzollini, & Severini, 2018) (Table 2).

In general, materials that are easier extruded are often printed at faster rates (Gillispie et al., 2020). Printing rate expresses the weight of the printed object over time Krishnaraj, Anukiruthika, Choudhary, Moses, & Anandharamakrishna, 2019; Theagarajan et al., 2020) (Table 2, equation 9), whereas extrusion rate evaluates the volume of the printed material over time (Theagarajan et al., 2020) (Table 2,

Table 2
Calculations employed in evaluation of print quality of cereal-based material.

Eq. No.	Parameter (symbol, unit)	Equation	Equation variables	Reference
1	Extruded length fraction (L_f, %)	$L_f = (L_{ext}/L_{input}) \times 100$ where $Lext = \sqrt{(x2-x1)2+(y2-y1)2}$	L_{ext} - *extruded line length, calculated from the x- and y-positions of the boundaries' extremities corresponding to the shortest length between the two matrix points;* L_{input} - *the theoretical line length*	Fahmy et al. (2020)
2	Oozing index (I_{ooze}, %)	$I_{ooze} = A_t/A_{Ti} \times 100$	A_t - *the area of the isolated region obtained after trapezoidal integration on the height distribution,* A_{Ti} - *theoretical area using the obtained average height*	
3	Fraction of the stable width (W_f)/heigh (H_f) (%)	$W_f = W_s/W_{input} \times 100$; H_f=(H_s/nozzle diameter) × 100	W_s - *stable width;* W_{input} - *theoretical length* H_s - *stable height*	
4	Line height (H, mm)	$H = (\sqrt{4w^2 - 16A + 4\pi A} - 2w)/(\pi\text{-}4)$ where $A = \frac{Q \times L_0}{L \times v}$	*w - measured mode line width, stable width (mm); A - calculated cross-sectional area; Q - volumetric flow rate (*mm^3/s*;* L_0 *- target line length (mm), L -measured line length (mm), v -printing speed (mm/s)*	Ma et al. (2021)
5	Printing precision (%) – *in relation to designed model*	$Dd = (D - D_0)/D_0 \times 100$ $Hd = (H - H_0)/H_0\ 100$	*D - measured diameter of printed samples;* D_0 *- designed diameter; H - measured thickness of printed samples;* H_0 *- designed thickness*	Huang et al. (2020)
6	Printing precision (%) – *in relation to nozzle diameter*	Printing precision = D_{wt} / D_{pn} × 100	D_{wt} - *diameter of the 3D-printed thread at the top after solidification;* D_{pn} - *diameter of the printing nozzle*	Habuš et al., 2021; Keerthana et al., 2020
7	Printing/Shape fidelity (%)	Printing fidelity = $(1 - \frac{\lvert Printed\ area - Designed\ area\rvert}{Designed\ area}) \times 100$ Shape fidelity = (Measured dimensions × 100)/Theoretical dimension		Vieira et al., 2020; Guo et al., 2021; Oliveira et al., 2022
8	Printing kinetics	$H_t/H_\infty = 1 - \exp(-k^*t)^n$	H_t *and* H_∞ *are the height of the printed product after time t and at the end of the printing process; k and n - coefficients.*	Derossi et al. (2018)
9	Printing rate (g/s)	Printing rate = w/t	*W - weight of printed object (g); t - time required to print sample (s)*	Krishnaraj et al., 2019; Theagarajan et al., 2020
10	Extrusion rate (ER, mm^3/s)	ER = Dn × h × Vn	*ER - volume of the extruded/deposited material for unit of time (*mm^3/s*); Dn -nozzle diameter (mm); h - layer height (mm); Vn - desired print speed (mm/s)*	Derossi et al., 2020b
11	Printing rate kinetics ($W_{(t)}$)	$W_{(t)} = k \times t$	$W_{(t)}$ *- weight of printed object in time t (g); t - time (s); k - rate constant (g/s)*	Derossi et al. (2018)
12	Shear rate ($\dot{\gamma}$, s^{-1})	$\dot{\gamma} = \frac{4Q}{\pi R^3}$	γ *- shear rate (*s^{-1}*), R - radius at the tip of the nozzle (mm), Q - flow rate (*mm^3/s*) determined using the mass flow and density of the material by printing for a specified time and measuring the weight of material that came out of the nozzle*	Heckl et al. (2022)

equation 10). Furthermore, printing rate kinetics can be obtained after fitting data to a common linear model (Derossi et al., 2018) (Table 2, equation 11). Shear rate can also be determined, as shown by Heckl et al. (2020) on the wheat starch-soy protein isolate ink using equation 12 (Table 2). Still, one should consider that shear rate during printing varies from point to point because of the syringe shape. Thus, viscosity values need to be put into the model of a dynamic form (Guo et al., 2020). The repeatability of printing can be estimated using analysis of variance for repeated measures considering the weight or line width of each printed shape printed from at least two syringe fillings. Namely, weight or volume of each subsequent printed object from the syringe can differ from the first printed shape (Vukušić Pavičić et al., 2021). With large-scale production, quality control including product dimensional analysis could be automated using machine vision (Akundi & Reyna, 2021).

4. Determination of end-product quality

After printing, cereal formulations generally require thermal post-processing such as cooking, baking, steaming or drying, to improve digestibility, sensory and nutritional properties. Stability and preservation of the 3D-printed structure during post-processing is challenging but crucial for the integration of 3D printing within traditional cooking techniques as well as its application in the food sector.

The quality of food includes many aspects, of which sensory and physical properties are the first steps in the development of new products. The most common physical properties of cereal foods are determined instrumentally. Structural deformation of cereal products in post-processing can be estimated as a change of its dimension after post-processing in a similar manner as for the shapes generated in printing (see Section 3). Dimensions, such as width, height, thickness or area, can be measured with a calliper or using digital image analysis of printed shape before and after post-processing. Deformation can be calculated using the equation $\Delta X\ (\%) = (X1 - X2) / X1 \times 100$, where X1 and X2 are dimensions or area before and after post-processing, respectively (Pulatsu et al., 2020). A positive value indicates a shrinkage in comparison to the printed shape, while a negative value implies a spreading (Habuš et al., 2021; Pulatsu et al., 2020). Although, spreading or shrinkage are common in conventional thermal processing of cereal material, it can be problematic in 3D printing integrated with thermal post-processing system.

Microscopic analysis can be used to evaluate the microstructure of the printed products by observing structural construction and layer deformity (Theagarajan et al., 2020). Scanning electron microscopy (SEM) has been used by several researchers to analyse the structural characteristics of various 3D-printed cereal-based snacks and cookies. These authors (Habuš et al., 2022a; Jo, Lim, Kim, & Park, 2021; Kim et al., 2019; Liu et al., 2020b; Liu et al., 2020a) used SEM at different magnifications (from 300× to 20,000×) to observe and analyse the microstructures of the printed products. Using the technique of SEM, the microstructures of 3D-printed snacks and cookies could be studied and structural constructions, layer deformations, porosity, compactness, convolutions, and changes in structure due to the addition of different ingredients could be observed. In addition, SEM enabled detailed images to be obtained and microstructural features to be analysed, providing insights into the printing performance, dimensional stability, product stability, and baking effects of the printed food products.

Methods such as flatbed scanning, X-ray microtomography, and micro-CT imaging, provided researchers non-destructive ways to study and quantify the microstructures of 3D-printed foods. Guénard-Lampron, Masson, Leichtnam, & Blumenthal (2021) used a flatbed scanner to acquire images of cut 3D-printed wheat flour-carrot puree cakes. The obtained full colour images with a resolution of 600 dpi were transformed using ImageJ software to determine the total area of pores. This method allowed the researchers to assess the relationship between total pore area, crust strength, firmness inside the cakes, and water loss during baking. Severini et al. (2018) estimated the microstructure of 3D-printed insect-enriched wheat snacks using X-ray microtomography. Cross-sections of the samples were used to reconstruct grayscale 3D images with Nrecon software. The images were then converted into binary form using an automatic thresholding algorithm. CTan software was employed to analyse the total porosity of the samples. Varghese et al. (2020) used a micro-CT imager to evaluate the microstructure (open porosity, closed porosity, and total porosity) of 3D-printed millet cookies. The raw image projections were reconstructed using a modified Feldkamp back-projection algorithm in the Nrecon software. Structural parameters were then analysed using CTan software. This method allowed the researchers to study the impact of infill density on porosity and to observe changes in the microstructure of the printed cookies. Derossi et al. (2020a, 2021) also employed a micro-CT imager to analyse printed wheat and rice flour snacks. CTan software was used to analyse the structural parameters. The researchers observed changes in pore size, number, and shape as a result of 3D printing, and also investigated how printing movements affected the positions of the pores.

Being one of the most important food properties for consumers' acceptance, food texture is the result of a complex system comprising of vision, hearing, touch, and kinaesthetic (Derossi et al., 2021). Derossi et al. (2021) defined hardness as the maximum force recorded during the compression test and the relative density of the snacks was found to affect their hardness. Severini et al. (2018) found also a direct relationship between the filling level, the solid fraction, and the hardness of 3D-printed snacks. The studies by Derossi et al. (2020a) and Lille et al. (2018) provided insights into the factors influencing the hardness of 3D-printed cereal-based snacks. The following critical factors were identified: (i) printing path; (ii) balance between printing speed and extrusion rate; (iii) compression of the food formula during extrusion. The hardness of 3D-printed snacks is commonly determined using a compression test (Table 3). Furthermore, the cutting test was proposed as a suitable method for measuring the hardness of snacks (Habuš et al., 2022a; Lille et al., 2018). This method involves cutting the snack and measuring the force required to cut through it. The 3-point bending test was also used to measure the hardness and fracturability of cookies (Jagadiswaran et al., 2021; Kim et al., 2019). In this test a force was applied to the cookie at three points, and the resulting deformation and force measurements provided information on the cookie's texture. Penetration tests have been applied to various cereal products to measure their texture properties (Table 3). This test involves penetrating a

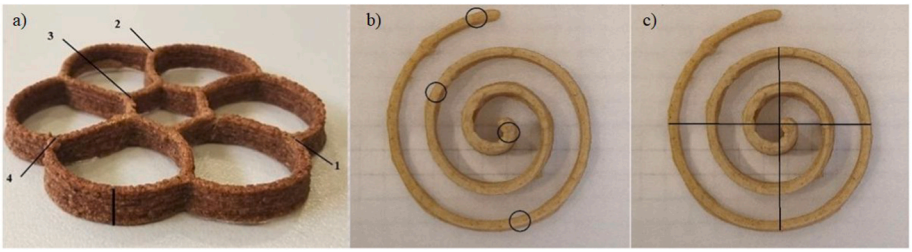

Fig. 2. Measurement positions of 3D-printed snacks height (a), height and line width (b), diameter (c) (from Habuš et al., 2022b; Vukušić Pavičić et al., 2021).

probe into the sample and measuring the force required to achieve a certain depth. It provides information on the sample's hardness and resistance to penetration. However, despite the variability of the available methods for measuring texture, there is a general need for their optimisation and further development, as the reported measurement deviations in the different tests are rather high (Habuš et al., 2022b; Lille et al., 2020).

Colour is an important attribute that determines consumer acceptance of a food product (Keerthana et al., 2020). Colorimeters have been used to assess the colour of different 3D-printed foods, such as microalga-enriched functional cookies (Vieira et al., 2020), high-fibre cookie formulations (Vukušić Pavičić et al., 2021), insect-enriched wheat flour snacks (Severini et al., 2018), wheat- and amaranth-bran snacks (Habuš et al., 2021; 2022b), and rice paste products (Liu et al., 2020b). The measurements were conducted using a black and white standard under artificial fluorescent light at room temperature. The colour difference (ΔE*) between samples, changes in colour during storage, and colour differences between the raw dough and thermally processed samples were determined using L* (lightness), a* (red-green), b* (yellow-blue) average values. Spectrophotometers were used for colour analysis of 3D-printed products, such as grape pomace-enriched wheat biscuits (Jagadiswaran et al., 2021), fibre-rich mung bean-millet snacks (Krishnaraj et al., 2019), and mushroom-enriched wheat flour snacks (Keerthana et al., 2020). Measurements were also expressed using the CIELab system, and in some cases the total colour difference (ΔE*) between samples and the browning index were calculated for the colour comparison between baked snacks and printed dough. These colour analysis methods enabled the measurement and comparison of colour attributes, such as L*, a*, and b*, C*ab (saturation), and hue angle (h°ab), providing information on the colour characteristics and changes in 3D-printed food products throughout various processes and storage periods.

Sensory analysis is a gold standard for evaluating the market potential of food products. Published studies used different methods and scales to evaluate sensory properties of 3D-printed cereal-based foods (Table 3). Most researchers employ a nine-point hedonic scale (from 1 = dislike extremely, to 9 = like extremely), following the ISO Standard 11035 (International Organization for Standardization, 2014), using a trained or semi-trained panel, usually consisting of 20 subjects (Table 3). Using this scale, attributes related to flavour, colour, taste, after-taste, aroma, appearance, thread quality, dimensional stability, texture, and overall acceptability were rated. In that manner, Krishnaraj et al. (2019) denoted the sensory score of 4 as the cut-off point for edibility and 5.5 considered as the cut-off point for marketability of 3D-printed snacks.

In the study by Habuš et al. (2022b), a 13-member panel of semi-trained participants evaluated the uniformity of surface colour, odour, and taste/flavour of 3D-printed snacks enriched with wheat and amaranth bran. The authors used a five-point hedonic scale, following ISO Standard No. 4121 (International Organization for Standardization, 2003). Jagadiswaran et al. (2021) conducted a preference test to narrow down the number of treatments analysed by the panellists in the acceptance test. Only the highly rated samples from the preference test were further examined. Oliveira et al. (2022) used a seven-point Likert scale in their sensory evaluation, which was performed by a 30-member untrained panel. The Likert scale is commonly used to measure respondents' agreement or preference with a set of statements or attributes. In the study by Oliveira et al. (2022), a CATA (check-all-that-apply) analysis was performed. The panellists were presented with a list of terms and asked to check all the terms they considered appropriate to describe each snack. Lille et al. (2020) used a descriptive method with a 10-member trained panel to rate the intensity of attributes related to appearance, texture, taste, and flavour. The panellists rated the attributes on a continuous graphical intensity scale ranging from 0 (attribute not existing) to 10 (attribute very clear). The sensory analysis methods described allowed the evaluation of various sensory attributes of the 3D-printed cereal-based foods, providing insights into consumers' perception and acceptance of these products. Reference should also be made to the International Dysphagia Diet Standardisation Initiative (IDDSI), which aims to develop international standardised terminology and definitions to describe texture-altered foods and thickened liquids. As 3D printing has great application potential to make texture-modified foods more appealing to patients with dysphagia (Lorenz, Iskandar, Baeghbali, Ngadi, & Kubow, 2022), sensory evaluation of cereal-based foods should also consider IDDSI terminology where appropriate.

5. Conclusions and suggestions for future research

A good understanding of the underlying mechanisms affecting 3D printing will enable forecasting of printing quality, but this can only be achieved by use of appropriate assessment techniques. Therefore, this review shows the commonly used methods in the development of cereal-based 3D-printed products up to date, summarizing common applications, identifying areas for improvement, and clarifying ambiguities in the terminology used. Methods include those that consider the quality of both the material and the printed raw object, as well as the final cereal products that underwent post-processing. This review made several aspects regarding assessment methods of cereal-based 3D-printed products evident:

1) Most studies involve dynamic rheological measurements of cereal-based inks to a lesser or greater extent, but they are rarely used for meaningful interpretation. Indeed, conditions in the rheometer are different from those in the extrusion-based 3D printer but rheological data can be used as predictors of printing outcomes, to a certain extent. In addition, deeper research and understanding of the structural properties of cereal-based raw materials should help to better predict the quality of printed products.
2) It is apparent that evaluation methods and related terminology are not uniformly used among researchers. The term printability is associated with various aspects of the process, such as extrudability, printing precision, accuracy and fidelity, which are not standardized in usage. This review suggests the use of the most common terminology, and defines it in detail, to avoid further overlap of methods and terms.
3) Evaluation of end-product quality is usually done following methods used for conventional cereal products, while there are only few attempts to extend the methods to better suit 3D-printed products. In example, texture analysis could be evolved to better suit 3D products by use of alternative analyser probes or test settings. Also, in sensory evaluation inclusion of descriptive methods beside hedonistic could better identify important features of 3D products.

Future studies should also focus on methods for determination undesirable but also intentional and controlled changes of colour, shape, and flavour of 3D-printed food over time which are of particular interest in 4D food printing.

CRediT authorship contribution statement

Nikolina Čukelj Mustač: Conceptualization, Visualization, Investigation, Writing – original draft, Writing – review & editing. **Kristian Pastor:** Investigation, Writing – original draft, Writing – review & editing. **Jovana Kojić:** Investigation, Writing – original draft, Writing – review & editing. **Bojana Voučko:** Visualization, Writing – original draft, Project administration. **Duška Ćurić:** Conceptualization, Writing – original draft, Supervision. **João Miguel Rocha:** Conceptualization, Writing – review & editing, Funding acquisition. **Dubravka Novotni:** Conceptualization, Visualization, Investigation, Writing – original draft, Writing – review & editing, Funding acquisition.

Table 3
Examples of instrumental texture measurement protocols and sensory evaluation protocols of cereal-based 3D-printed products.

3D-printed product	Test type	Measuring system	Attributes	Reference
Instrumental protocols using texture analyser				
Wheat/millet-based snacks	texture profile analysis	double compression test with P/75, P/5 pre-test speed of 1–1.5 mm/s, test speed of 1 mm/s, post-speed of 10 mm/s, compression of 50% of the initial height of the samples	hardness, chewiness, cohesiveness, springiness	Derossi et al., 2020a; Krishnaraj et al., 2019
Cereal-based cookies/snacks	compression, puncture (penetration)	probe diameter of 1.7–6 mm; compression until 50% of initial diameter; trigger force of 5 g up to 90% strain level; pre-test speed of 1–1.5 mm/s, test speed of 1–5 mm/s, post-test speed of 10 mm/s	hardness, breaking strength, fracturability	Severini et al., 2018; Varghese et al., 2020; Jo et al., 2021; Vieira et al., 2020; Derossi et al., 2021; Uribe-Wandurraga et al., 2020
Cookies with grape pomace or hydrocolloids	three-point bending	3-point bend rig with a target distance of 20.0 mm and a test speed of 1.0 mm/s	hardness, fracturability	Jagadiswaran et al., 2021; Kim et al., 2019
Wheat protein/fiber enriched snacks	cutting	knife blade at a speed of 1–3 mm/s and post-speed of 5 mm/s	hardness	Keerthana et al., 2020; Lille et al., 2018; Habuš et al., 2022a; 2022b
Sensory evaluation protocols				
Enriched wheat and millet cookies/ snacks; Rice starch paste	Hedonic 9-point; preference ranking and acceptance tests; ISO 11035	20 semi-trained panellists	Appearance, Colour, Dimensional stability, Shape Layer definitions, Texture, Thread quality, Taste, Flavour, After-taste, Aroma, Overall acceptability	Jagadiswaran et al., 2021; Theagarajan et al., 2020; Krishanraj et al., 2019; Keerthana et al., 2020
Wheat- and amaranth-bran enriched snacks	Hedonic 5-point; ISO 4121	13 semi-trained panellists	Surface colour, Odour, Taste/flavour	Habuš et al. (2022b)
Enriched rye snack	Descriptive analysis; ISO 6658:2017	10 trained panellists	Appearance, Texture, Taste, Flavor	Lille et al. (2020)
Enriched oat flour snacks	7-point Likert scale liking; preference test	30 untrained panelists	Colour, Appearance, Aroma, Texture, Flavor, Global appreciation, Purchase intention	Oliveira et al. (2022)
Enriched oat flour snacks	Check-all-that-apply (CATA) analysis	30 untrained panelists	30 descriptors: Appearance (4), Texture (4), Aroma (8), Flavor (9), Taste (3), Intensity of aftertaste (2)	Oliveira et al. (2022)

Declaration of competing interest

The authors declare that they have no known competing financial interests or personal relationships that could have appeared to influence the work reported in this paper.

Data availability

No data was used for the research described in the article.

Acknowledgements

This research was done under the Croatian Science Foundation project [IP-2020-02-3829] and Provincial Secretariat for Higher Education and Scientific Research of Republic of Serbia [142-451-3125/2023-01/01]. Any opinions, findings, conclusions, or recommendations expressed in this material are those of the authors and do not necessarily reflect the views of the Croatian Science Foundation.

This work is based upon the work from COST Action 18101 SOURDOMICS - *Sourdough biotechnology network towards novel, healthier and sustainable food and bioprocesses* (https://sourdomics.com/; https://www.cost.eu/actions/CA18101/), where J.M.R. is the Chair of the Action, N.C.M. is DCEB and WG 7 member, D.N. is Management Committee member and WG 4 vice-leader, K.P. is WG 4 leader and B.V. is member of WG 2 and 4. SOURDOMICS are supported by COST (European Cooperation in Science and Technology). COST is a funding agency for research and innovation networks. COST Actions help connect research initiatives across Europe and enable scientists to grow their ideas by sharing them with their peers-thus boosting their research, career and innovation.

References

Akundi, A., & Reyna, M. (2021). A machine vision based automated quality control system for product dimensional analysis. *Procedia Computer Science, 185*, 127–134. https://doi.org/10.1016/j.procs.2021.05.014

Cheng, Y., Fu, Y., Ma, L., Yap, P. L., Losic, D., Wang, H., et al. (2022). Rheology of edible food inks from 2D/3D/4D printing, and its role in future 5D/6D printing. *Food Hydrocolloids*. , Article 107855. https://doi.org/10.1016/j.foodhyd.2022.107855

Derossi, A., Caporizzi, R., Azzollini, D., & Severini, C. (2018). Application of 3D printing for customized food. A case on the development of a fruit-based snack for children. *Journal of Food Engineering, 220*, 65–75. https://doi.org/10.1016/j.jfoodeng.2017.05.015

Derossi, A., Caporizzi, R., Oral, M. O., & Severini, C. (2020a). Analyzing the effects of 3D printing process per se on the microstructure and mechanical properties of cereal

food products. *Innovative Food Science & Emerging Technologies, 66*, Article 102531. https://doi.org/10.1016/j.ifset.2020.102531
Derossi, A., Caporizzi, R., Paolillo, M., & Severini, C. (2021). Programmable texture properties of cereal-based snack mediated by 3D printing technology. *Journal of Food Engineering, 289*, Article 110160. https://doi.org/10.1016/j.jfoodeng.2020.110160
Derossi, A., Caporizzi, R., Ricci, I., & Severini, C. (2019). Critical variables in 3D food printing. In F. Godoi, B. Bhandari, S. Prakash, & M. Zhang (Eds.), *Fundamentals of 3D food printing and applications* (pp. 41–91). Academic Press. https://doi.org/10.1016/B978-0-12-814564-7.00003-1.
Derossi, A., Paolillo, M., Caporizzi, R., & Severini, C. (2020b). Extending the 3D food printing tests at high speed. Material deposition and effect of non-printing movements on the final quality of printed structures. *Journal of Food Engineering, 275*, Article 109865. https://doi.org/10.1016/j.jfoodeng.2019.109865
Fahmy, A. R., Becker, T., & Jekle, M. (2020). 3D printing and additive manufacturing of cereal-based materials: Quality analysis of starch-based systems using a camera-based morphological approach. *Innovative Food Science & Emerging Technologies, 63*, Article 102384. https://doi.org/10.1016/j.ifset.2020.102384
Gillispie, G., Prim, P., Copus, J., Fisher, J., Mikos, A. G., Yoo, J. J., et al. (2020). Assessment methodologies for extrusion-based bioink printability. *Biofabrication, 12* (2), Article 022003. https://doi.org/10.1088/1758-5090/ab6f0d
Guénard-Lampron, V., Masson, M., Leichtnam, O., & Blumenthal, D. (2021). Impact of 3D printing and post-processing parameters on shape, texture and microstructure of carrot appetizer cake. *Innovative Food Science & Emerging Technologies, 72*, Article 102738. https://doi.org/10.1016/j.ifset.2021.102738
Guo, C., Zhang, M., & Devahastin, S. (2020). 3D extrusion-based printability evaluation of selected cereal grains by computational fluid dynamic simulation. *Journal of Food Engineering, 286*, Article 110113. https://doi.org/10.1016/j.jfoodeng.2020.110113
Guo, C., Zhang, M., & Devahastin, S. (2021). Improvement of 3D printability of buckwheat starch-pectin system via synergistic Ca2+-microwave pretreatment. *Food Hydrocolloids, 113*, Article 106483. https://doi.org/10.1016/j.foodhyd.2020.106483
Habuš, M., Benković, M., Iveković, D., Pavičić, T. V., Mustač, N.Č., Voučko, B., et al. (2022a). Effect of oil content and enzymatic treatment on dough rheology and physical properties of 3D-printed cereal snack. *Journal of Cereal Science, 108*, Article 103559. https://doi.org/10.1016/j.jcs.2022.103559
Habuš, M., Golubić, P., Vukušić Pavičić, T., Čukelj Mustač, N., Voučko, B., Herceg, Z., et al. (2021). Influence of flour type, dough acidity, printing temperature and bran pre-processing on browning and 3D printing performance of snacks. *Food and Bioprocess Technology, 14*(12), 2365–2379. https://doi.org/10.1007/s11947-021-02732-w
Habuš, M., Mykolenko, S., Iveković, S., Pastor, K., Kojić, J., Drakula, S., et al. (2022b). Bioprocessing of wheat and amaranth bran for the reduction of fructan levels and application in 3D-printed snacks. *Foods, 11*(11), 1649. https://doi.org/10.3390/foods11111649
Heckl, M. P., Korber, M., Jekle, M., & Becker, T. (2023). Relation between deformation and relaxation of hydrocolloids-starch based bio-inks and 3D printing accuracy. *Food Hydrocolloids, 137*, Article 108326. https://doi.org/10.1016/j.foodhyd.2022.108326
Huang, C. Y. (2018). *Extrusion-based 3D printing and characterization of edible materials*. Waterloo, ON, Canada: Master's Thesis, University of Waterloo. http://hdl.handle.net/10012/12899, 14th of March 2023.
Huang, M. S., Zhang, M., & Bhandari, B. (2019). Assessing the 3D printing precision and texture properties of brown rice induced by infill levels and printing variables. *Food and Bioprocess Technology, 12*, 1185–1196. https://doi.org/10.1007/s11947-019-02287-x
Huang, M. S., Zhang, M., & Guo, C. F. (2020). 3D printability of brown rice gel modified by some food hydrocolloids. *Journal of Food Processing and Preservation, 44*(7), Article e14502. https://doi.org/10.1111/jfpp.14502
International Organization for Standardization. (2003). *Sensory analysis — guidelines for the use of quantitative response scales*. ISO Standard No.121:2003) https://www.iso.org/standard/33817.html.
International Organization for Standardization. (2014). *Sensory analysis—identification and selection of descriptors for establishing a sensory profile by a multidimensional approach*. ISO Standard No. 11035:1994) https://www.iso.org/standard/19015.html.
Jagadiswaran, B., Alagarasan, V., Palanivelu, P., Theagarajan, R., Moses, J. A., & Anandharamakrishnan, C. (2021). Valorization of food industry waste and by-products using 3D printing: A study on the development of value-added functional cookies. *Future Foods, 4*, Article 100036. https://doi.org/10.1016/j.fufo.2021.100036
Ji, S., Xu, T., Li, Y., Li, H., Zhong, Y., & Lu, B. (2022). Effect of starch molecular structure on precision and texture properties of 3D printed products. *Food Hydrocolloids, 125*, Article 107387. https://doi.org/10.1016/j.foodhyd.2021.107387
Ji, S., Zeng, Q., Xu, M., Li, Y., Xu, T., Zhong, Y., et al. (2023). Investigation of the mechanism of different 3D printing performance of starch and whole flour gels from tuber crops. *International Journal of Biological Macromolecules, 241*, Article 124448. https://doi.org/10.1016/j.ijbiomac.2023.124448
Jo, G. H., Lim, W. S., Kim, H. W., & Park, H. J. (2021). Post-processing and printability evaluation of red ginseng snacks for three-dimensional (3D) printing. *Food Bioscience, 42*, Article 101094. https://doi.org/10.1016/j.fbio.2021.101094
Keerthana, K., Anukiruthika, T., Moses, J. A., & Anandharamakrishnan, C. (2020). Development of fiber-enriched 3D printed snacks from alternative foods: A study on button mushroom. *Journal of Food Engineering, 287*, Article 110116. https://doi.org/10.1016/j.jfoodeng.2020.110116
Kim, H. W., Lee, I. J., Park, S. M., Lee, J. H., Nguyen, M. H., & Park, H. J. (2019). Effect of hydrocolloid addition on dimensional stability in post-processing of 3D printable cookie dough. *Lebensmittel-Wissenschaft & Technologie, 101*, 69–75. https://doi.org/10.1016/j.lwt.2018.11.019
Krishnaraj, P., Anukiruthika, T., Choudhary, P., Moses, J. A., & Anandharamakrishnan, C. (2019). 3D extrusion printing and post-processing of fibre-rich snack from indigenous composite flour. *Food and Bioprocess Technology, 12* (10), 1776–1786. https://doi.org/10.1007/s11947-019-02336-5
Lille, M., Kortekangas, A., Heiniö, R. L., & Sozer, N. (2020). Structural and textural characteristics of 3D-printed protein-and dietary fibre-rich snacks made of milk powder and wholegrain rye flour. *Foods, 9*(11), 1527. https://doi.org/10.3390/foods9111527
Lille, M., Nurmela, A., Nordlund, E., Metsä-Kortelainen, S., & Sozer, N. (2018). Applicability of protein and fiber-rich food materials in extrusion-based 3D printing. *Journal of Food Engineering, 220*, 20–27. https://doi.org/10.1016/j.jfoodeng.2017.04.034
Liu, Z., Bhandari, B., Prakash, S., Mantihal, S., & Zhang, M. (2019). Linking rheology and printability of a multicomponent gel system of carrageenan-xanthan-starch in extrusion based additive manufacturing. *Food Hydrocolloids, 87*, 413–424. https://doi.org/10.1016/j.foodhyd.2018.08.026
Liu, Y., Tang, T., Duan, S., Qin, Z., Li, C., Zhang, Z., et al. (2020a). Effects of sodium alginate and rice variety on the physicochemical characteristics and 3D printing feasibility of rice paste. *Lebensmittel-Wissenschaft & Technologie, 127*, Article 109360. https://doi.org/10.1016/j.lwt.2020.109360
Liu, Y., Tang, T., Duan, S., Qin, Z., Zhao, H., Wang, M., et al. (2020b). Applicability of rice doughs as promising food materials in extrusion-based 3D printing. *Food and Bioprocess Technology, 13*, 548–563. https://doi.org/10.1007/s11947-020-02415-y
Lorenz, T., Iskandar, M. M., Baeghbali, V., Ngadi, M. O., & Kubow, S. (2022). 3D food printing applications related to dysphagia: A narrative review. *Foods, 11*(12), 1789. https://doi.org/10.3390/foods11121789
Maldonado-Rosas, R., Tejada-Ortigoza, V., Cuan-Urquizo, E., Mendoza-Cachú, D., Morales-de La Pena, M., Alvarado-Orozco, J. M., et al. (2022). Evaluation of rheology and printability of 3D printing nutritious food with complex formulations. *Additive Manufacturing, 58*, Article 103030. https://doi.org/10.1016/j.addma.2022.103030
Masbernat, L., Berland, S., Leverrier, C., Moulin, G., Michon, C., & Almeida, G. (2021). Structuring wheat dough using a thermomechanical process, from liquid food to 3D-printable food material. *Journal of Food Engineering, 310*, Article 110696. https://doi.org/10.1016/j.jfoodeng.2021.110696
Ma, Y., Schutyser, M. A., Boom, R. M., & Zhang, L. (2021). Predicting the extrudability of complex food materials during 3D printing based on image analysis and gray-box data-driven modelling. *Innovative Food Science & Emerging Technologies, 73*, Article 102764. https://doi.org/10.1016/j.ifset.2021.102764
Mezger, T. G. (2015). In *Applied rheology: With Joe flow on rheology road* (6th ed.). Anton Paar GmbH.
Nijdam, J. J., Agarwal, D., & Schon, B. S. (2021). Assessment of a novel window of dimensional stability for screening food inks for 3D printing. *Journal of Food Engineering, 292*, Article 110349. https://doi.org/10.1016/j.jfoodeng.2020.110349
Oliveira, S., Sousa, I., & Raymundo, A. (2022). Printability evaluation of Chlorella vulgaris snacks. *Algal Research, 68*, Article 102879. https://doi.org/10.1016/j.algal.2022.102879
Pulatsu, E., Su, J. W., Lin, J., & Lin, M. (2020). Factors affecting 3D printing and post-processing capacity of cookie dough. *Innovative Food Science & Emerging Technologies, 61*, Article 102316. https://doi.org/10.1016/j.ifset.2020.102316
Radoš, K., Benković, M., Mustač, N.Č., Habuš, M., Voučko, B., Pavičić, T. V., et al. (2023). Powder properties, rheology and 3D printing quality of gluten-free blends. *Journal of Food Engineering, 338*, Article 111251. https://doi.org/10.1016/j.jfoodeng.2022.111251
Sahin, S., & Sumnu, S. G. (2006). *Physical properties of foods*. Springer Science & Business Media. https://doi.org/10.1007/0-387-30808-3
Severini, C., Azzollini, D., Albenzio, M., & Derossi, A. (2018). On printability, quality and nutritional properties of 3D printed cereal based snacks enriched with edible insects. *Food Research International, 106*, 666–676. https://doi.org/10.1016/j.foodres.2018.01.034
Theagarajan, R., Moses, J. A., & Anandharamakrishnan, C. (2020). 3D extrusion printability of rice starch and optimization of process variables. *Food and Bioprocess Technology, 13*, 1048–1062. https://doi.org/10.1007/s11947-020-02453-6
Uribe-Wandurraga, Z. N., Zhang, L., Noort, M. W., Schutyser, M. A., García-Segovia, P., & Martínez-Monzó, J. (2020). Printability and physicochemical properties of microalgae-enriched 3D-printed snacks. *Food and Bioprocess Technology, 13*, 2029–2042. https://doi.org/10.1007/s11947-020-02544-4
Varghese, C., Wolodko, J., Chen, L., Doschak, M., Srivastav, P. P., & Roopesh, M. S. (2020). Influence of selected product and process parameters on microstructure, rheological, and textural properties of 3D printed cookies. *Foods, 9*(7), 907. https://doi.org/10.3390/foods9070907
Vieira, M. V., Oliveira, S. M., Amado, I. R., Fasolin, L. H., Vicente, A. A., Pastrana, L. M., et al. (2020). 3D printed functional cookies fortified with Arthrospira platensis: Evaluation of its antioxidant potential and physical-chemical characterization. *Food Hydrocolloids, 107*, Article 105893. https://doi.org/10.1016/j.foodhyd.2020.105893
Vukušić Pavičić, T., Grgić, T., Ivanov, M., Novotni, D., & Herceg, Z. (2021). Influence of flour and fat type on dough rheology and technological characteristics of 3D-printed cookies. *Foods, 10*(1), 193. https://doi.org/10.3390/foods10010193
Zhang, J. Y., Pandya, J. K., McClements, D. J., Lu, J., & Kinchla, A. J. (2022). Advancements in 3D food printing: A comprehensive overview of properties and opportunities. *Critical Reviews in Food Science and Nutrition, 62*(17), 4752–4768. https://doi.org/10.1080/10408398.2021.1878103